MANTRA: AN INTEGRAL REACTOR PHYSICS EXPERIMENT TO INFER ACTINIDE CAPTURE CROSS-SECTIONS FROM *THORIUM* TO *CALIFORNIUM* WITH ACCELERATOR MASS SPECTROMETRY

FCRD group meeting, June 24-25, 2010, Port Jefferson, NY

G. Youinou[2], H. Walk[2], R. Vondrasek[1], M. Salvatores[2,4], B. Scott[1], E. Rehm[1], M. Paul[1], R. Pardo[1], G. Palmiotti[2], C. Nair[1], J.K. Nimmagadda[3] , M. Meyer[2], C. McGrath[2], S. Kondrashev[1], F. Kondev[1], G. Imel[3], C. Glass[2], C. Clark[2]

[1] Argonne National Laboratory

[2] Idaho National Laboratory

[3] Idaho State University

[4] CEA-Cadarache

Principle of the experiment:

1 – Irradiate very pure actinide material (a few mg) in well-characterized neutron spectra in the Advanced Test Reactor (**ATR**) at INL

→ ^{232}Th, ^{235}U, ^{236}U, ^{238}U, ^{237}Np, ^{238}Pu, ^{239}Pu, ^{240}Pu, ^{241}Pu, ^{242}Pu, ^{241}Am, ^{243}Am, ^{244}Cm and ^{248}Cm

2 – Measure the atom densities of the transmutation products with Accelerator Mass Spectrometry at the **ATLAS** facility at ANL

→ detection limit of AMS is orders of magnitude lower than that of standard MS (~10^{-12})

→ more transmutation products can be measured

→ more neutron cross-sections to be inferred from a single sample

3 – Measure the neutron fluence in the actinide samples

→ ^{148}Nd and ^{137}Cs in ^{235}U monitors

4 – Infer the effective neutron capture cross-sections from results of step 2 and 3

Relation between measured and inferred quantities

$$\frac{d\,N_A^Z(t)}{dt} = -N_A^Z(t)\,\tilde{\sigma}_{A,Z}^a(t)\,\phi(t)$$

$$\frac{d\,N_{A+1}^Z(t)}{dt} = +N_A^Z(t)\,\bar{\sigma}_{A,Z}^c(t)\,\phi(t) - N_{A+1}^Z(t)\,\tilde{\sigma}_{A+1,Z}^a(t)\,\phi(t)$$

$$\frac{d\,N_{A+2}^Z(t)}{dt} = +N_{A+1}^Z(t)\,\bar{\sigma}_{A+1,Z}^c(t)\,\phi(t) - N_{A+2}^Z(t)\,\tilde{\sigma}_{A+2,Z}^a(t)\,\phi(t)$$

$$\frac{d\,N_{A+3}^Z(t)}{dt} = +N_{A+2}^Z(t)\,\bar{\sigma}_{A+2,Z}^c(t)\,\phi(t) - N_{A+3}^Z(t)\,\tilde{\sigma}_{A+3,Z}^a(t)\,\phi(t)$$

.....

Inferred quantities Measured quantities

$$\bar{\sigma}_{A+k}^c(t) = \frac{\int \sigma_{A+k}^c(E)\,\varphi(E,t)\,dE}{\int \varphi(E,t)\,dE}$$ = effective neutron capture cross-section

$$\tilde{\sigma}_{A+k}^a = \bar{\sigma}_{A+k}^c + \bar{\sigma}_{A+k}^f + \frac{\lambda_{A+k}}{\phi}$$ = effective neutron absorption cross-section + natural decay

Relation between measured and inferred quantities

Example of A+1, A+2 and A+3 build-up from successive captures on mass number A

$$N_A(T) = N_A(0)\, e^{-\tilde{\sigma}_A^a \bar{\phi}\, T} \sim N_A(0)[1 - \tilde{\sigma}_A^a \bar{\phi}\, T]$$

$$N_{A+1}(T) = N_A(0)\, \bar{\sigma}_A^c \left(\frac{e^{-\tilde{\sigma}_A^a \bar{\phi}\, T}}{\tilde{\sigma}_{A+1}^a - \tilde{\sigma}_A^a} + \frac{e^{-\tilde{\sigma}_{A+1}^a \bar{\phi}\, T}}{\tilde{\sigma}_A^a - \tilde{\sigma}_{A+1}^a} \right) \sim N_A(0)\, \bar{\sigma}_A^c \bar{\phi}\, T$$

$$N_{A+2}(T) = N_A(0)\, \bar{\sigma}_A^c \bar{\sigma}_{A+1}^c \left(\frac{e^{-\tilde{\sigma}_A^a \bar{\phi}\, T}}{(\tilde{\sigma}_{A+1}^a - \tilde{\sigma}_A^a)(\tilde{\sigma}_{A+2}^a - \tilde{\sigma}_A^a)} + \frac{e^{-\tilde{\sigma}_{A+1}^a \bar{\phi}\, T}}{(\tilde{\sigma}_A^a - \tilde{\sigma}_{A+1}^a)(\tilde{\sigma}_{A+2}^a - \tilde{\sigma}_{A+1}^a)} + \frac{e^{-\tilde{\sigma}_{A+2}^a \bar{\phi}\, T}}{(\tilde{\sigma}_A^a - \tilde{\sigma}_{A+2}^a)(\tilde{\sigma}_{A+1}^a - \tilde{\sigma}_{A+2}^a)} \right)$$

$$\sim \frac{1}{2} N_A(0)\, \bar{\sigma}_A^c\, \bar{\sigma}_{A+1}^c [\bar{\phi}\, T]^2$$

$$N_{A+3}(T) = N_A(0)\, \bar{\sigma}_A^c \bar{\sigma}_{A+1}^c \bar{\sigma}_{A+2}^c \left(\frac{e^{-\tilde{\sigma}_A^a \bar{\phi}\, T}}{(\tilde{\sigma}_{A+1}^a - \tilde{\sigma}_A^a)(\tilde{\sigma}_{A+2}^a - \tilde{\sigma}_A^a)(\tilde{\sigma}_{A+3}^a - \tilde{\sigma}_A^a)} + \frac{e^{-\tilde{\sigma}_{A+1}^a \bar{\phi}\, T}}{(\tilde{\sigma}_A^a - \tilde{\sigma}_{A+1}^a)(\tilde{\sigma}_{A+2}^a - \tilde{\sigma}_{A+1}^a)(\tilde{\sigma}_{A+3}^a - \tilde{\sigma}_{A+1}^a)} + \frac{e^{-\tilde{\sigma}_{A+2}^a \bar{\phi}\, T}}{(\tilde{\sigma}_A^a - \tilde{\sigma}_{A+2}^a)(\tilde{\sigma}_{A+1}^a - \tilde{\sigma}_{A+2}^a)(\tilde{\sigma}_{A+3}^a - \tilde{\sigma}_{A+2}^a)} + \frac{e^{-\tilde{\sigma}_{A+3}^a \bar{\phi}\, T}}{(\tilde{\sigma}_A^a - \tilde{\sigma}_{A+3}^a)(\tilde{\sigma}_{A+1}^a - \tilde{\sigma}_{A+3}^a)(\tilde{\sigma}_{A+2}^a - \tilde{\sigma}_{A+3}^a)} \right)$$

$$\sim \frac{1}{6} N_A(0)\, \bar{\sigma}_A^c\, \bar{\sigma}_{A+1}^c\, \bar{\sigma}_{A+2}^c [\bar{\phi}\, T]^3$$

Relation between measured and inferred quantities

$$\bar{\sigma}_A^c \sim \frac{[\mathcal{N}_{A+1}(T)]_m - [\mathcal{N}_{A+1}(0)]_m}{[\bar{\phi}\, T]_m}$$

$$\bar{\sigma}_{A+1}^c \sim 2\frac{[\mathcal{N}_{A+2}(T)]_m - [\mathcal{N}_{A+2}(0)]_m}{\left([\mathcal{N}_{A+1}(T)]_m + [\mathcal{N}_{A+1}(0)]_m\right)[\bar{\phi}\, T]_m}$$

$$\bar{\sigma}_{A+2}^c \sim 3\frac{\left([\mathcal{N}_{A+3}(T)]_m - [\mathcal{N}_{A+3}(0)]_m\right)\left([\mathcal{N}_{A+1}(T)]_m + [\mathcal{N}_{A+1}(0)]_m\right)}{\left[[\mathcal{N}_{A+1}(T)]_m\left([\mathcal{N}_{A+2}(T)]_m + 2[\mathcal{N}_{A+2}(0)]_m\right) + [\mathcal{N}_{A+1}(0)]_m\left(2[\mathcal{N}_{A+2}(T)]_m + [\mathcal{N}_{A+2}(0)]_m\right)\right][\bar{\phi}\, T]_m}$$

$$\left([\mathcal{N}_{A+n}]_m = \frac{[N_{A+n}]_m}{[N_A]_m}\right)$$

Idaho National Laboratory

Relation between measured and inferred quantities

If $N(T) >> N(0)$ the expressions are simpler and the inference is less dependant on the precision of the measurement of the atom densities. Relatively easy with thermal or epithermal neutron spectra ($\bar{\sigma}^c$ ~ few 10 to few 100 barns). More difficult with fast neutron spectra ($\bar{\sigma}^c$~ 1 barn).

→ High neutron fluence

→ High purity samples

$$\bar{\sigma}_A^c \sim \frac{[\mathcal{N}_{A+1}(T)]_m - [\mathcal{N}_{A+1}(0)]_m}{[\bar{\phi}\,T]_m} \quad \Rightarrow \quad \bar{\sigma}_A^c \sim \frac{[\mathcal{N}_{A+1}(T)]_m}{[\bar{\phi}\,T]_m}$$

$$\bar{\sigma}_{A+1}^c \sim 2\frac{[\mathcal{N}_{A+2}(T)]_m - [\mathcal{N}_{A+2}(0)]_m}{\left([\mathcal{N}_{A+1}(T)]_m + [\mathcal{N}_{A+1}(0)]_m\right)[\bar{\phi}\,T]_m} \quad \Rightarrow \quad \bar{\sigma}_{A+1}^c \sim 2\frac{[\mathcal{N}_{A+2}(T)]_m}{[\mathcal{N}_{A+1}(T)]_m\,[\bar{\phi}\,T]_m}$$

$$\bar{\sigma}_{A+2}^c \sim 3\frac{\left([\mathcal{N}_{A+3}(T)]_m - [\mathcal{N}_{A+3}(0)]_m\right)\left([\mathcal{N}_{A+1}(T)]_m + [\mathcal{N}_{A+1}(0)]_m\right)}{\left[[\mathcal{N}_{A+1}(T)]_m\left([\mathcal{N}_{A+2}(T)]_m + 2[\mathcal{N}_{A+2}(0)]_m\right) + [\mathcal{N}_{A+1}(0)]_m\left(2[\mathcal{N}_{A+2}(T)]_m + [\mathcal{N}_{A+2}(0)]_m\right)\right][\bar{\phi}\,T]_m}$$

$$\Rightarrow \quad \bar{\sigma}_{A+2}^c \sim 3\frac{[\mathcal{N}_{A+3}(T)]_m}{[\mathcal{N}_{A+2}(T)]_m\,[\bar{\phi}\,T]_m}$$

Best sample candidates for ATLAS = Heaviest long-lived isotope in each element (U, Np, Pu, Am, Cm) because A+1, A+2… contamination can be kept at a much lower level

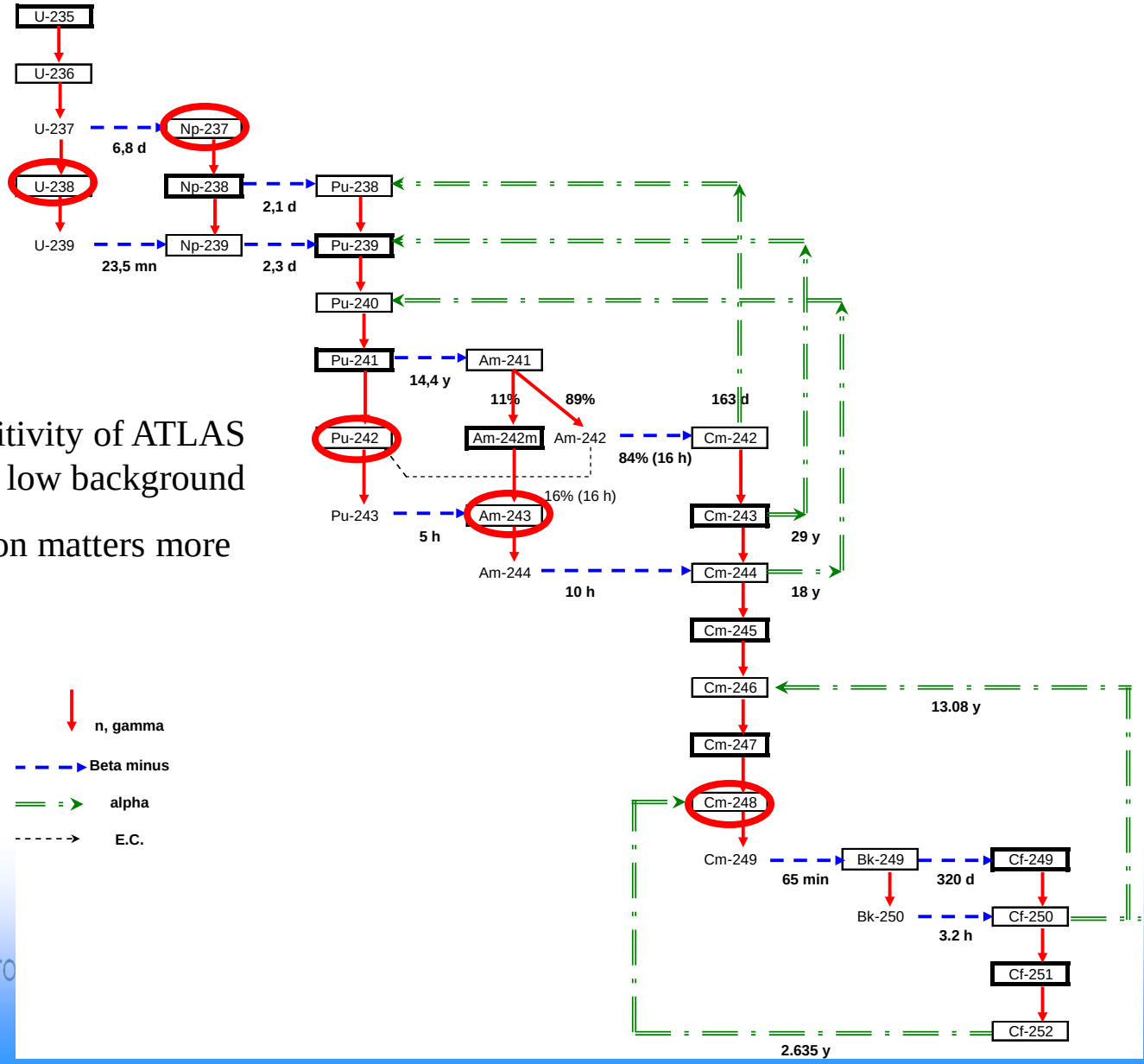

- For these samples the high sensitivity of ATLAS is an important asset because of a low background
- When high background, precision matters more than sensitivity

Idaho National Laborato

Neutron Fluence

Determination of the neutron fluence by the Nd-148 and Cs-137 method in U-235 monitors

U5	Th2	U5	U8	U5	Np7	U5	Pu2	U5	Am3	U5	Cm8	U5

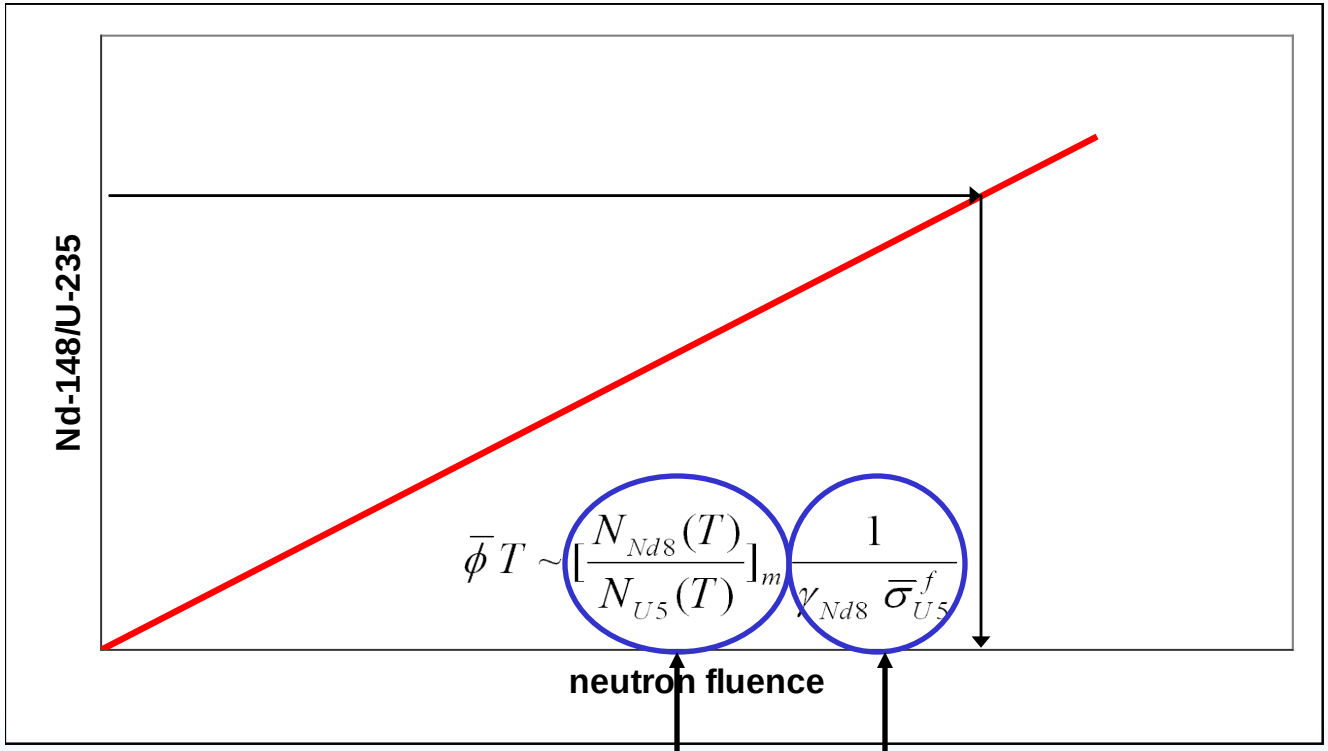

measured calculated

A Brief Description of ATR

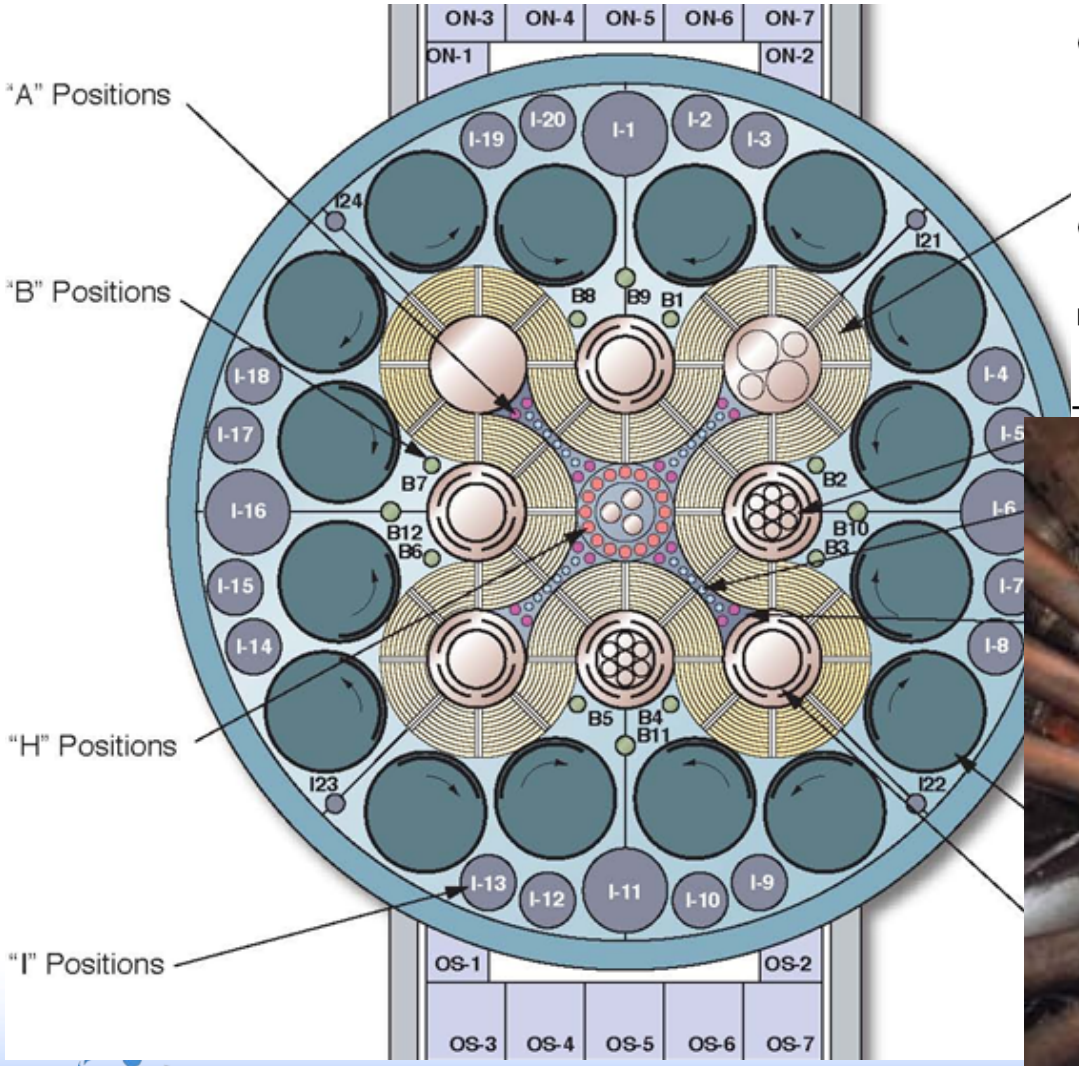

Reactor:	
Thermal power	250 MW_{th}[a]
Power density	1.0 MW/L
Maximum thermal neutron flux	1.0×10^{15} n/cm^2-sec[b]
Maximum fast flux	5.0×10^{14} n/cm^2-sec[b]
Number of flux traps	9
Number of experiment positions	68[c]
Core:	
Number of fuel assemblies	40
Active length of assemblies	4 feet
Number of fuel plates per assembly	19
Uranium-235 content of an assembly	1,075 g
Total core load	43 kg[d]
Coolant:	
Design pressure	2.7 Mpa (390 psig)
Design temperature	115°C (240°F)
Reactor Coolant:	
Light water maximum coolant flow ra	3.09 m^3/s (49,000 gpm)
Coolant temperature (operating)	<52°C (125°F) inlet, 71°C (160°F) outlet

Samples irradiation in ATR

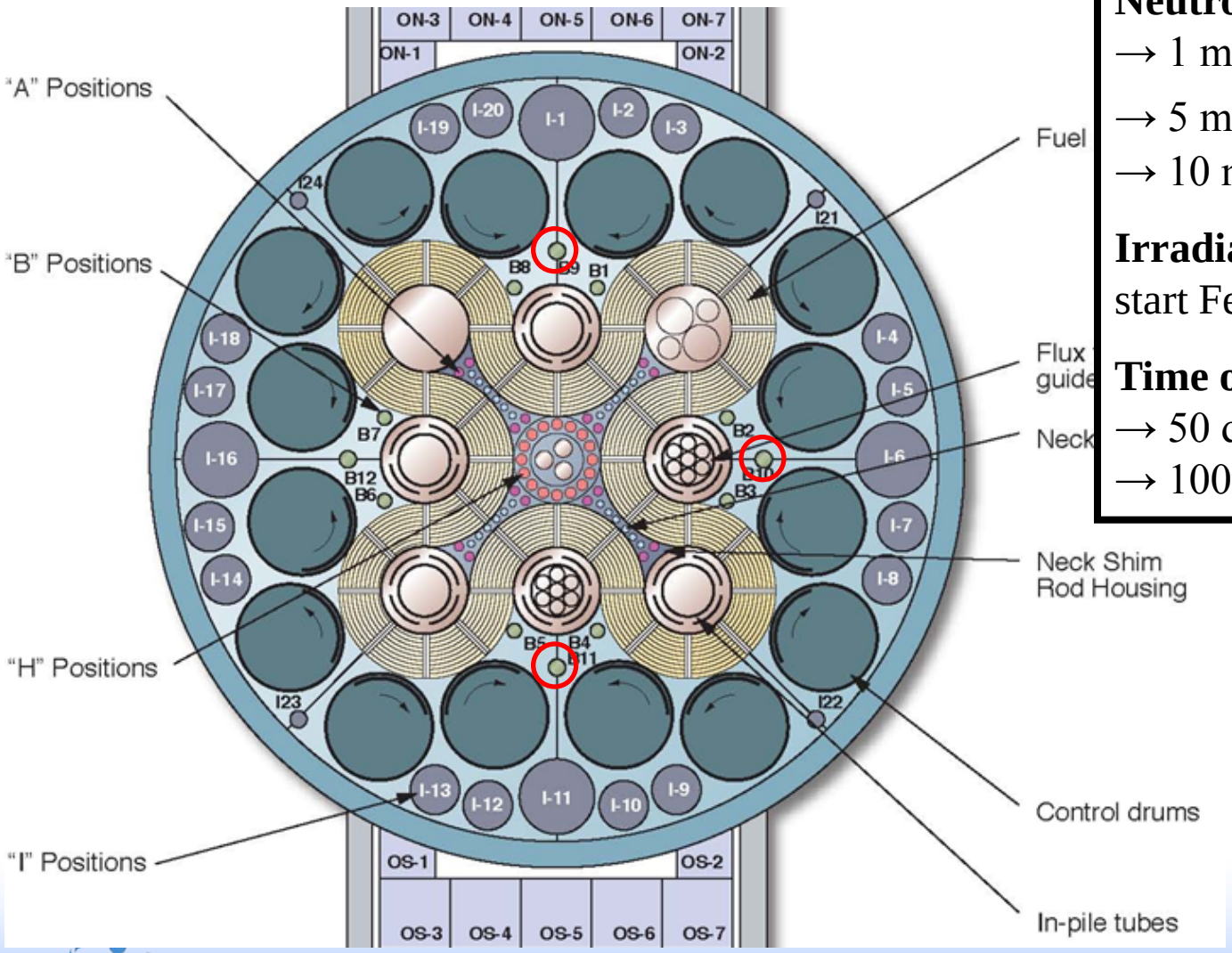

Positions:
→ B9, 10 and 11

Neutron filters:
→ 1 mm Cadmium
→ 5 mm Boron (70% ^{10}B)
→ 10 mm Boron (70% ^{10}B)

Irradiation: →
start February 2011

Time of irradiation:
→ 50 days for Cd-filter
→ 100 days for B-filtered

Samples irradiation in ATR

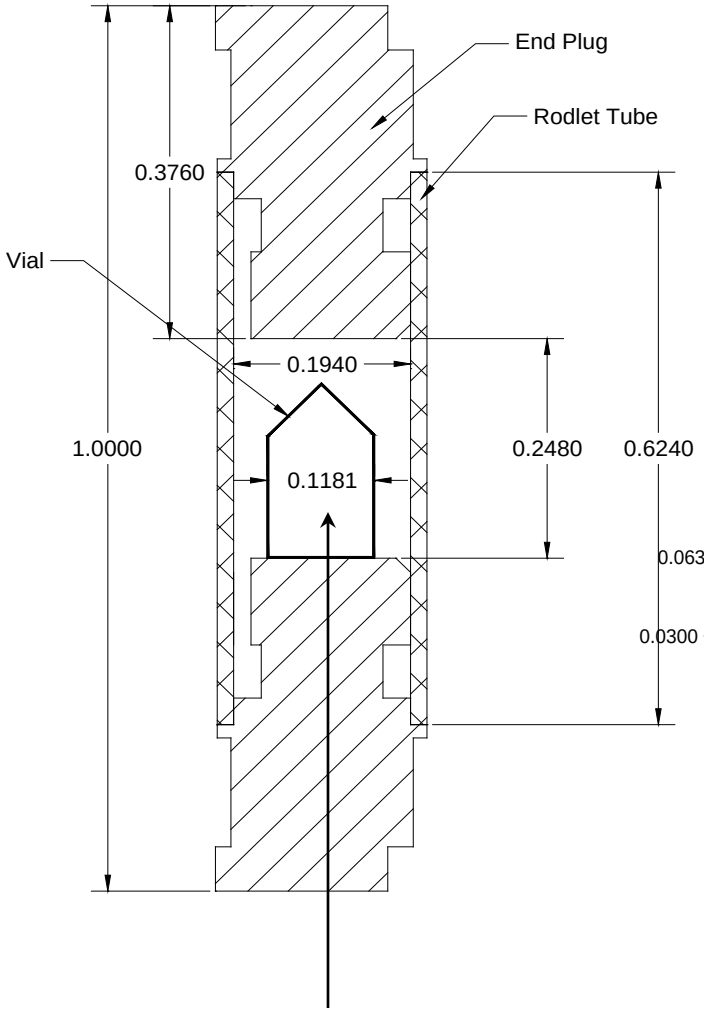

Actinide sample

Example of a boron filtered setup

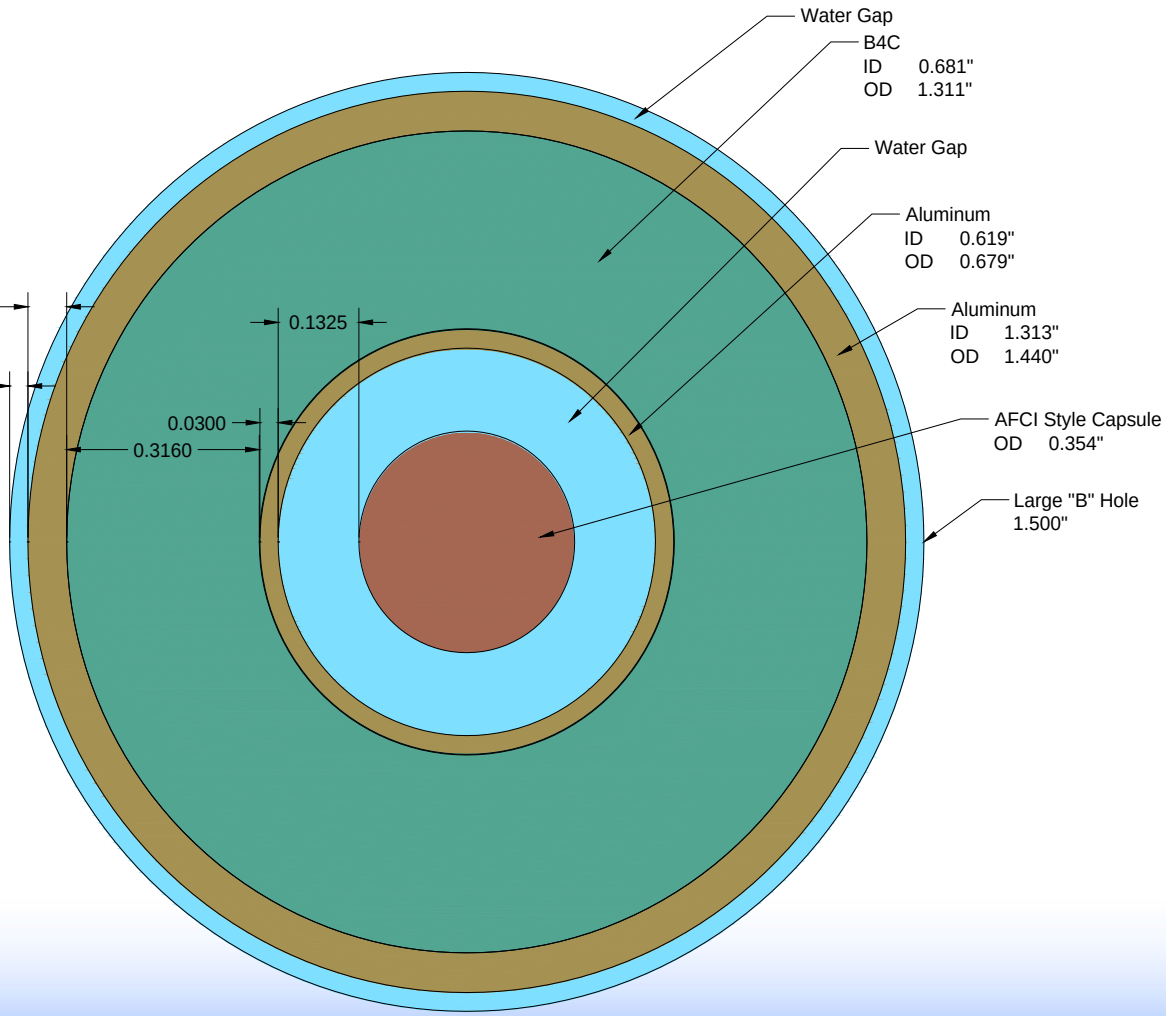

(C. Clark, INL, personal communication)

Idaho National Laboratory

Samples irradiation in ATR – Neutron filters

- The Cd neutron filter can be manufactured at the INL.

- Ceradyne, Inc identified as proposed vendor for B4C filters (70% ^{10}B)
  → SoW for B4C procurement to be sent before end of June (5-6 month lead time)

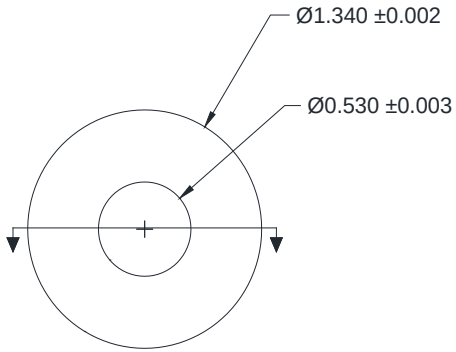

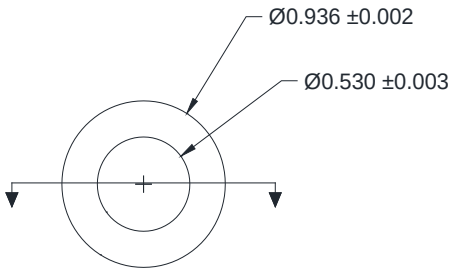

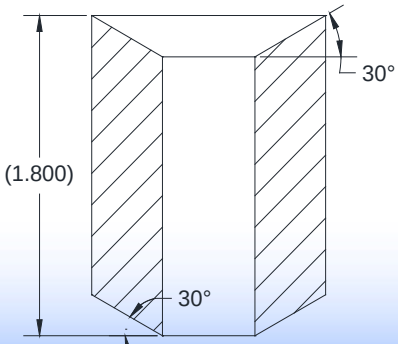

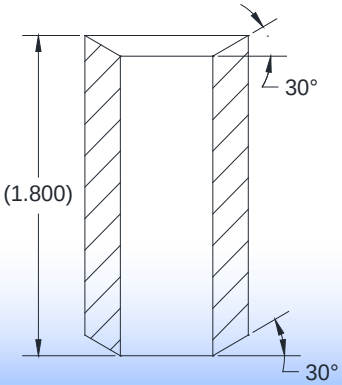

Idaho National Laboratory

Standard Pellet

Effect of neutron filters on the neutron spectrum in the samples

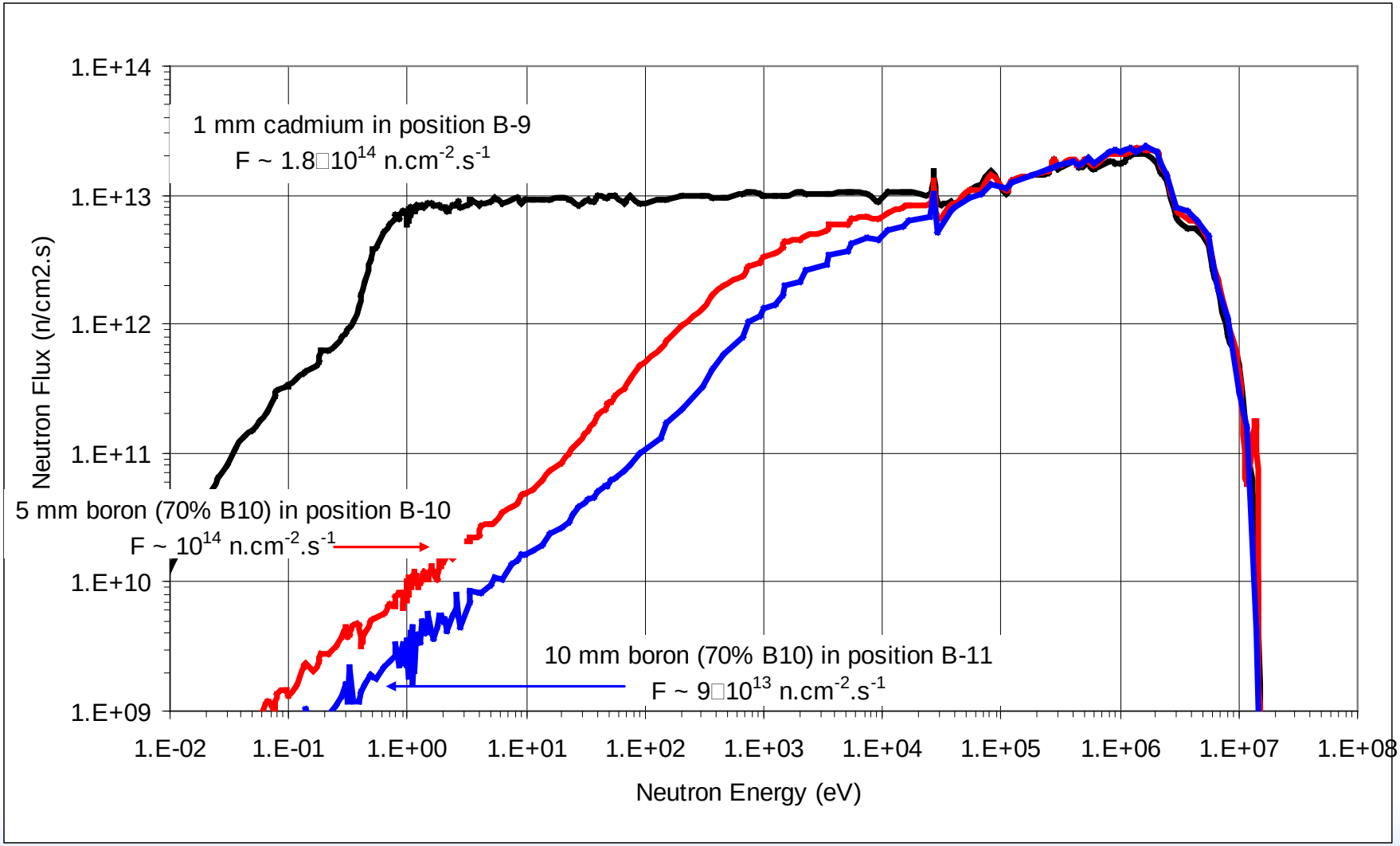

Idaho National Laboratory

(C. Glass, INL, personal communication)

Effect of neutron filters on the neutron spectrum in the samples

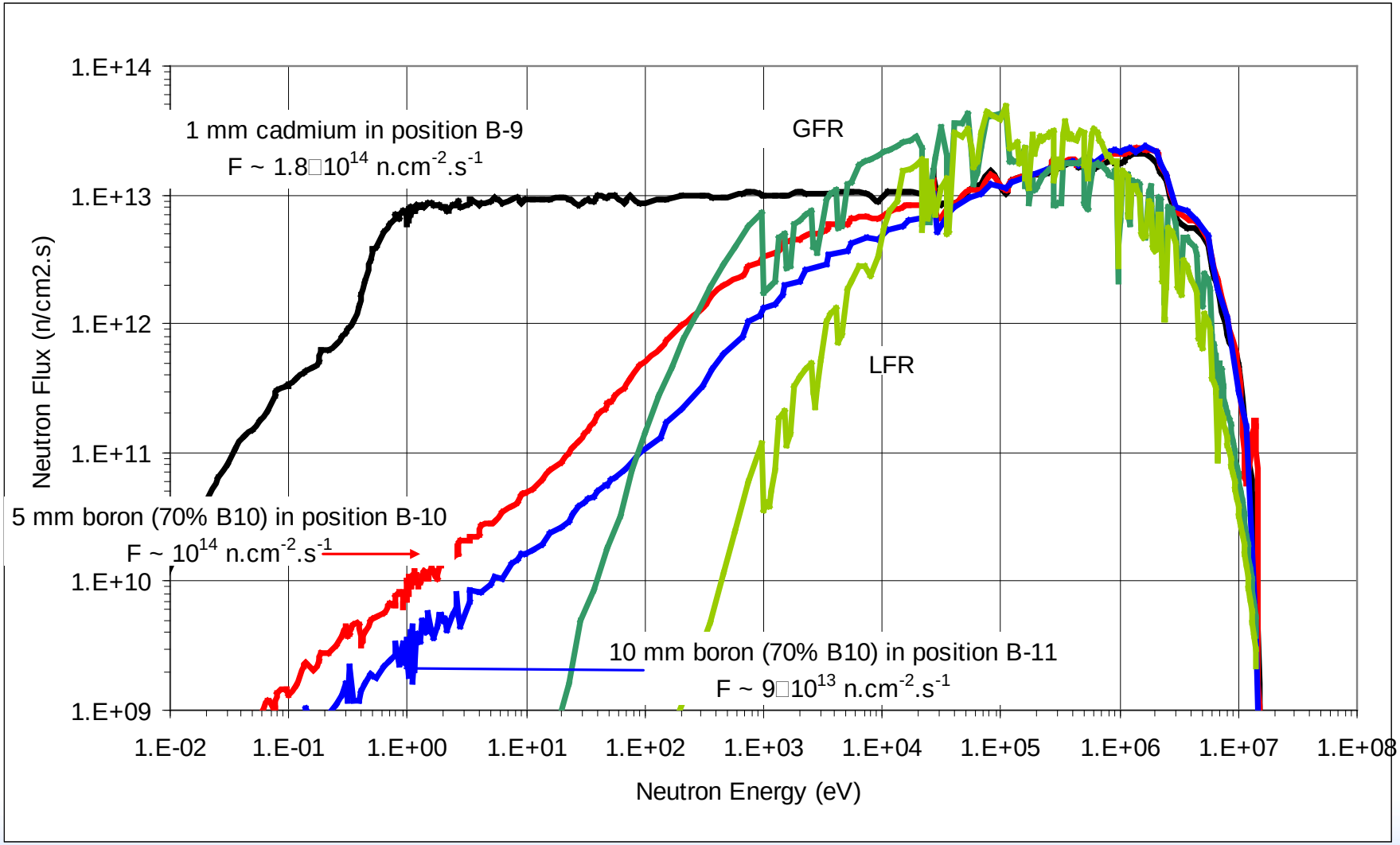

Idaho National Laboratory

(C. Glass, G. Palmiotti, INL, personal communication)

Effect of neutron filters on the neutron spectrum in the samples

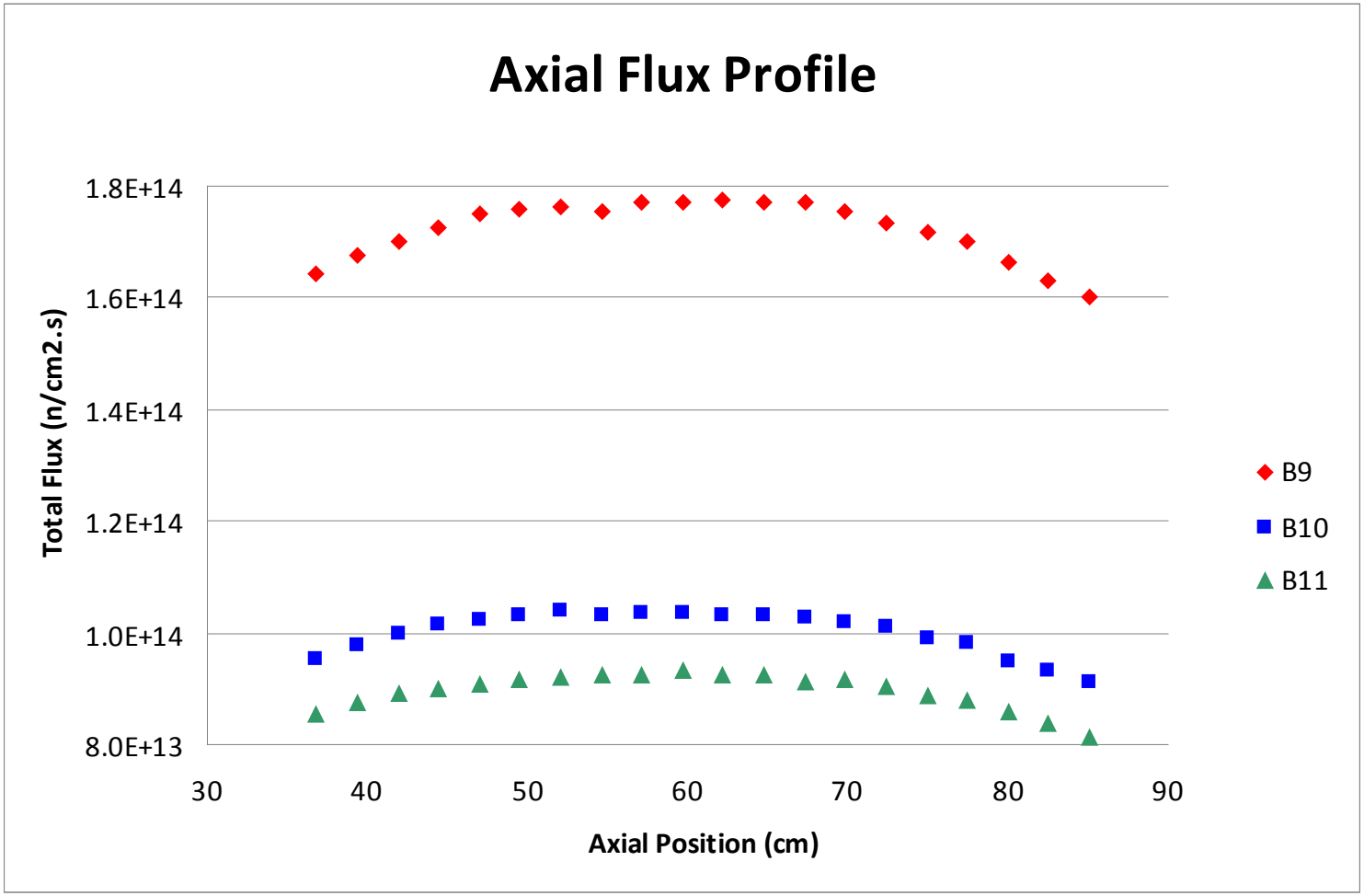

(C. Glass, INL, personal communication)

Idaho National Laboratory

Example of U-238, Pu-242 and Cm-248 samples (100% pure)

	U8	Pu9	Pu0	Pu1	Pu2	Am3	Cm2
50 days Cadmium	0.991	8E-03	2E-05	2E-06	2E-09	2E-11	1E-11
100 days Boron	0.999	2E-04	7E-08	2E-11	-	-	-

	Pu2	Am3	Cm4	Cm5	Cm6	Cm7
50 days Cadmium	0.964	3E-02	9E-04	6E-06	5E-09	4E-12
100 days Boron	0.999	3E-04	1E-07	2E-11	-	-

	Cm8	Bk9	Cf9	Cf0	Cf1	Cf2
50 days Cadmium	0.992	7E-03	4E-04	1E-04	8E-06	7E-08
100 days Boron	0.999	1E-04	3E-05	2E-07	1E-10	-

ATLAS

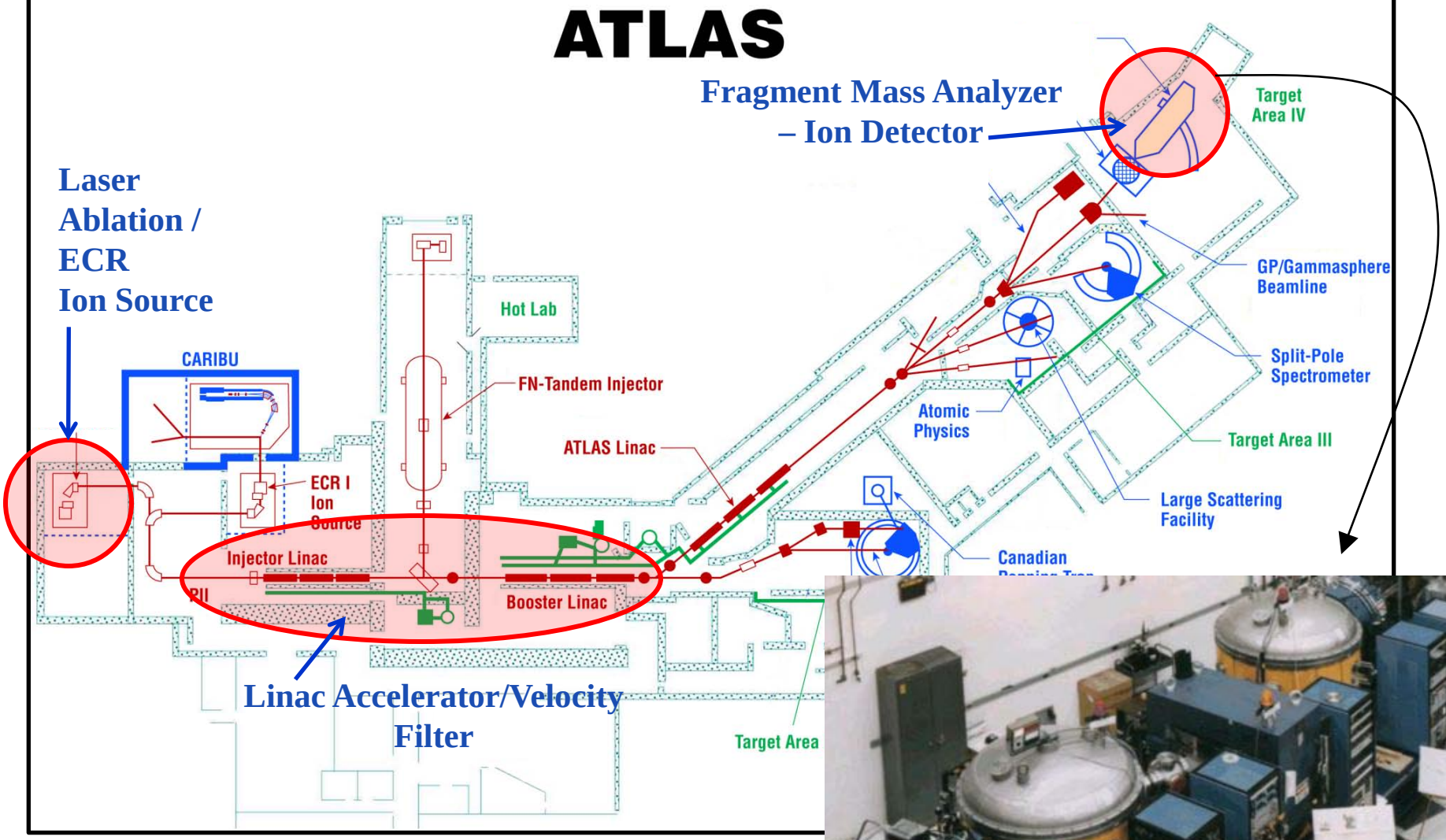

(R. Pardo, ANL, personal communication)

Idaho National Laboratory

Example of a FMA Focal Plane Spectrum for ^{236}U AMS

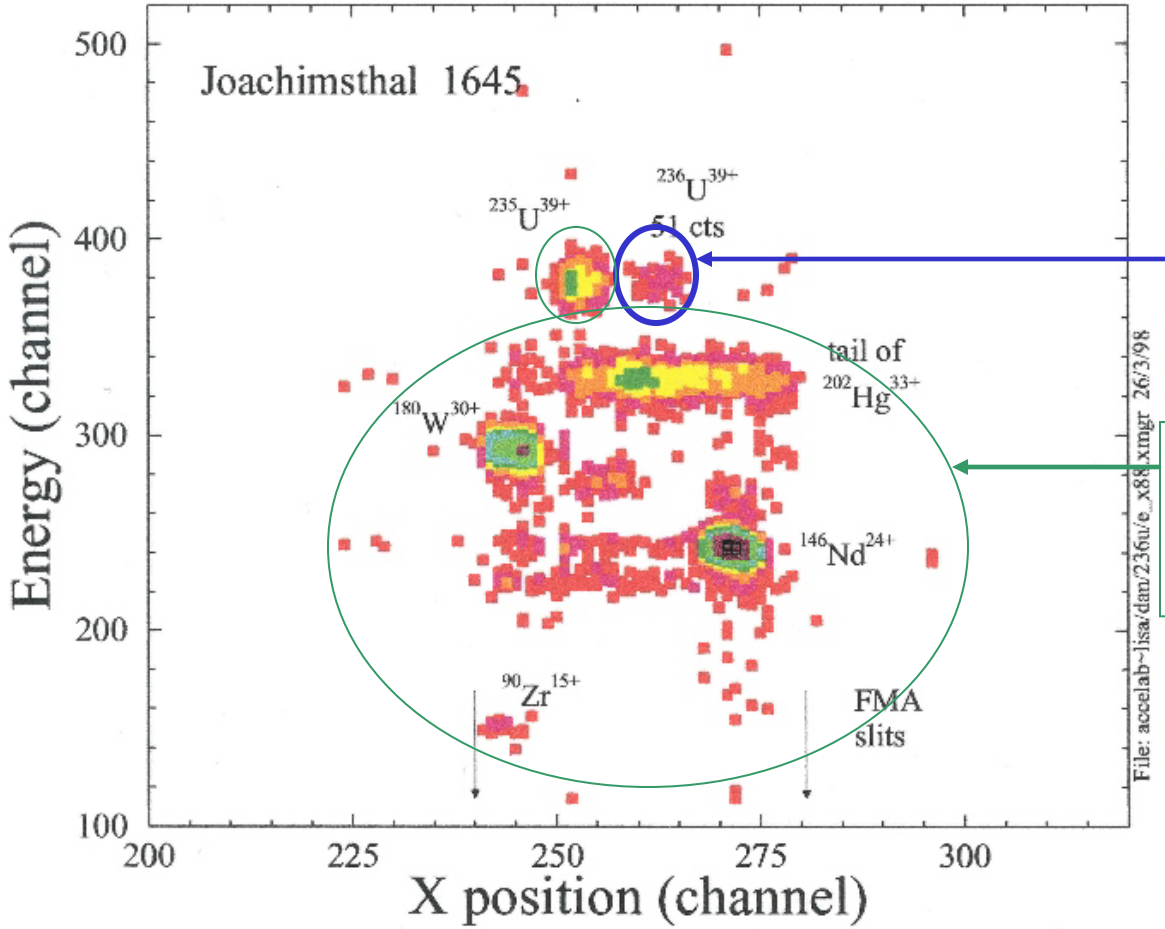

^{236}U cts (ion of interest)

m/q = 236/39

Ions with m/q = 236/39 δ (structural material + cross-talk from previous runs + ^{235}U)

Isotope spectrum at the FMA focal plane detector for a sample from the Joachimsthal mine – Measurement time ~ 10 min – $^{236}U/U \sim 1x10^{-10}$

(M. Paul, NIMB, B172, (2000) 688-692)

Idaho National Laboratory

Accuracy/Precision

1. Only 14C AMS routinely operates in the <1-2% range.
2. Relies on:
   - Dedicated facility
   - Absolute calibration standards
   - Rapid cycling between counted species and reference species
   - Rapid cycling between unknowns and standards
3. Must also minimize cross talk between samples
   - Laser ablation
   - Quartz liner
4. Focus is to know and track transmission

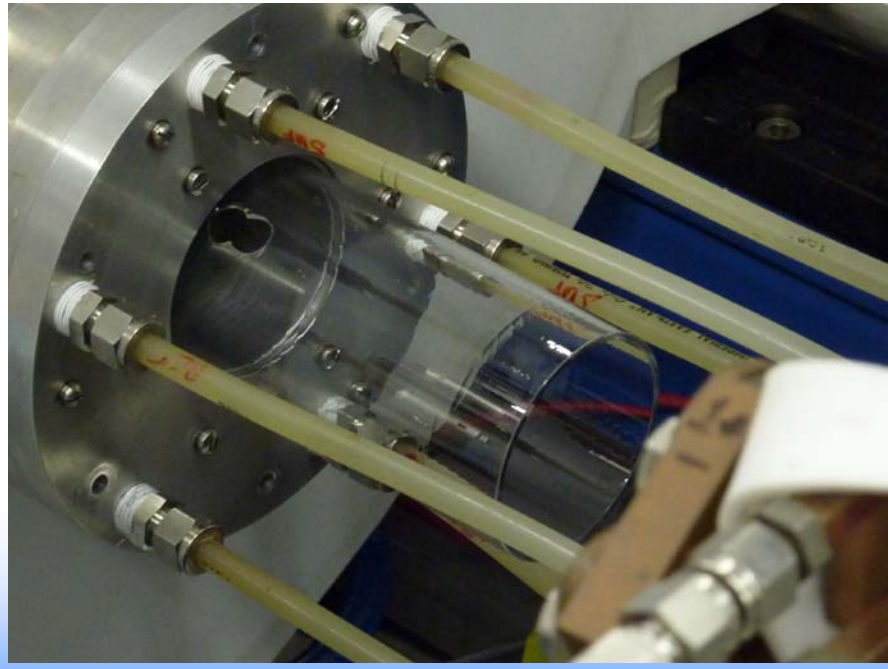

$$\frac{C_{A+1}}{C_A} = \frac{N_{A+1}}{N_A} \times \frac{T_{A+1}}{T_A}$$

Ratio of A+1 and A counts

Actual isotopic ratio in the sample

Ratio of the accelerator transmission for A and A+1

Optical Lay-out

Laser parameters:

- ❑ beam ∅ ~ 5 mm
- ❑ λ ~ 1000 nm
- ❑ E ~ 10 mJ/pulse
- ❑ Pulse width ~ 8 ps
- ❑ Focal spot ~ 0.4 mm → 10 J/cm²

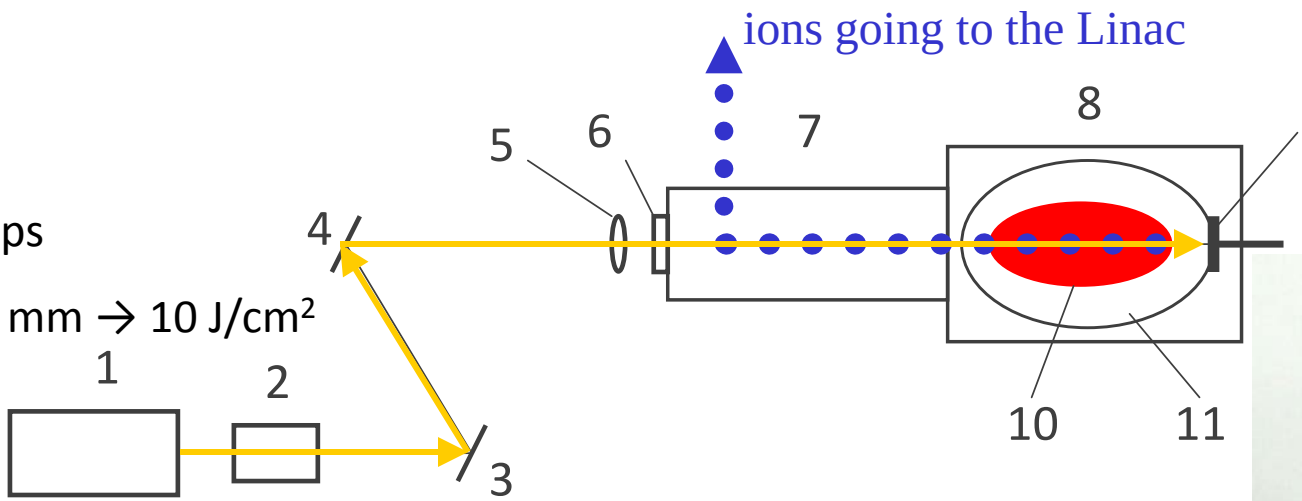

1 – laser, 2 – beam expander (3:1), 3 and 4 – plane mirrors, 5 – focusing lens, 6 – input window, 7 – ion beam transport pipe, 8 – ECR source chamber, 9 - sample with holder, 10 – ECR plasma area, 11- ablated material cloud

First tests with laser scheduled for the end of the summer 2010

(S. Kondrashev, ANL, personal communication)

Conclusions

- ❑ Integral reactor physics experiment under way to infer actinide capture cross-sections from Th to Cf in three neutron spectra from epithermal to fast
- ❑ Irradiation in ATR scheduled for Feb. 2011
- ❑ First AMS runs with un-irradiated samples scheduled for Feb. 2011 and with irradiated samples for October 2011
- ❑ Significant upgrades are under way at ATLAS to increase its performances
- ❑ Results in September 2012!

Acknowledgements

This work is supported by the U.S. Department of Energy, Office of Science, Office of Nuclear Physics, under DOE Idaho Operations Office Contract DE-AC07-05ID14517 as well as by the ANL Contract DE-AC02-06CH11357 and by the ATR National Scientific User Facility.

Advantages of Laser Ablation vs Sputtering or Oven Technique

- Any solid material (metal, isolator, semiconductor) can be used
- Small amount of sample material can be fed into the source
- Feeding of material from sample holder is avoided
- Material is emitted preferentially perpendicular to sample surface
- Reliable control of ablated material amount by changing laser beam energy and focal spot size

Choice of Laser

A psec pulse-length laser will be used to minimize throw-out of the molten material during ablation process.

In comparison with nsec pulse length laser:

- Lower contamination of ECR vacuum chamber from materials previously used
- Better control of ablated material amount